Environment and Natural Resources Journal

Volume 24
Issue X
2026

Analyzing the Seasonal Relationship between Vegetation Variation and Land Surface Temperature Dynamics in Eastern Maharashtra

Dipti Pawade[1,2*] and Sonali Patil[1]

[1]*Department of Information Technology, K J Somaiya School of Engineering, Somaiya Vidyavihar University, Vidyavihar, Mumbai, India*
[2]*Department of Computer Science and Engineering, Indian Institute of Information Technology, Nagpur, India*

ARTICLE INFO

Received: 28 Aug 2025
Received in revised: 15 Jan 2026
Accepted: 26 Jan 2026
Published online: 3 Apr 2026
DOI: 10.32526/ennrj/24/20250231

Keywords:
Normalized Difference Vegetation Index (NDVI)/ Land surface temperature/ Environment/ Land use land cover (LULC)/ NDVI and LST correlation

*** Corresponding author:**
E-mail:
dipti.pawade@somaiya.edu

ABSTRACT

Understanding land surface temperature (LST) change trend is very important in Eastern part of Maharashtra state, India as this region is undergoing rapid land-use change. Vegetation plays a critical role in regulating land surface temperature in such region. The main objective of this study is to analyze the vegetation change trend and investigate the seasonal relationship between vegetation variation and land surface temperature fluctuation from the years 2014 to 2022. Using Landsat 8 satellite imagery, the Normalized Difference Vegetation Index (NDVI) is derived to monitor vegetation variation and thermal infrared (TIR) bands is used to calculate LST. The methodology is divided into data collection, preprocessing, NDVI and LST calculation. Based on NDVI and adaptive vegetation classification, land use (LU) classification is carried out and finally correlation analysis between the various classes of LU, NDVI value with LST is calculated. The results suggest a clear seasonal pattern where the post-monsoon period has higher average NDVI values and lower average LST values as compared to the pre-monsoon periods. There was a declining trend of overall vegetation health throughout the study period, although 2022 showed a slight recovery in pre-season NDVI and improved vegetative health in post-monsoon dense vegetation classes. Correlation analyses consistently indicated a moderate-strong negative association (~ -0.2 to -0.5) of LST with vegetation cover (vegetation cooling effect) and a positive association (~ 0.1 to 0.5) with built-up areas (urban heat island effect). It highlights the importance of vegetation cover for local temperature management and has significant implications for the assessment of recent changes in the local environment.

HIGHLIGHTS

- Seasonal NDVI-LST dynamics were assessed using multi-temporal Landsat-8 data from 2014 to 2022.
- Adaptive NDVI percentile classification captured seasonal vegetation variability effectively.
- Post-monsoon periods showed higher NDVI values with consistently lower surface temperatures.
- NDVI showed a strong negative correlation with LST, confirming cooling effects.

1. INTRODUCTION

Ecologists and environmental scientists have consistently raised concern about global warming and its far-reaching effects (Li et al., 2025). Global warming leads to a temperature rise, which in turn causes the melting of glaciers, a rise in seawater levels, etc. (Venkataramanan and Smitha, 2011). While examining the adverse consequences of global warming, it is equally essential to analyze its anthropogenic and natural drivers. Out of all the driving factors, loss of vegetation is the primary cause of global warming (Longobardi et al., 2016). Plants and forests are crucial in regulating the Earth's weather patterns, as they absorb carbon dioxide from the air through photosynthesis and act as a carbon sink (Nassif et al., 2023). Expanding urban areas, infrastructure development, industrialization, and deforestation have had severe consequences on vegetation cover locally as well as globally (Pawade and Patil, 2025; Zhan et al., 2013). From an environmental perspective, this mechanism leads to massive imbalances within local ecosystems while limiting the planet's natural ability to

Citation: Pawade D, Patil S. Analyzing the seasonal relationship between vegetation variation and land surface temperature dynamics in Eastern Maharashtra. Environ. Nat. Resour. J. 2026;24(X):xx-xx.

capture carbon emissions (Psistaki et al., 2024). Moreover, this phenomenon simultaneously affects land surface temperature (LST) (Li et al., 2023). Through evapotranspiration, vegetation helps to moderate the land surface temperature. Evapotranspiration is a combination of two processes: evaporation of land water into vapor and transpiration, where water vapor is released from plants during photosynthesis. The vegetation loss diminishes the natural cooling mechanism, resulting in increased heat absorption by bare soil and built-up surfaces, which typically have lower albedo and higher heat retention (Islam et al., 2024). Consequently, areas with sparse vegetation tend to experience significantly higher land surface temperatures, especially during the day (Wei et al., 2025).

Many studies have been done focusing on local as well as global changes in the temperature and its driving factors (Bandh et al., 2021; De Frenne et al., 2021; Yuxi et al., 2024). In that regard, (Rahimi et al., 2025) derived the global correlation between Normalized Difference Vegetation Index (NDVI) and LST, using Moderate Resolution Imaging Spectroradiometer (MODIS) satellite data. While offering valuable global insights, the research identifies the need for higher-resolution data, an understanding of seasonal variations, and the assessment of extreme climate event impacts to provide better analysis. (Kumar and Shekhar, 2015) investigated the similar relationship for Kalaburagi City, India. Finding highlighted a negative correlation with green spaces and a positive correlation with the Normalized Difference Build-up Index (NDBI). The study acknowledged the unavailability of in-situ LST measurements as limitation. Another study (Ullah et al., 2023) comprehensively analyzes the relationships between LST, Land Use Land Cover (LULC), NDVI, and topographic elements in the Lower Himalayan region. This study is focused on a multi-dimensional spatial analysis. The key finding underscores the relationship between elevation and LST. The LST decreases with elevation while built-up areas exhibiting the highest LST. LULC misclassification errors inherent by Maximum Likelihood Classification (MLC) method hampered the accuracy for few classes, despite its overall good accuracy. Researchers (Alademomi et al., 2022) further investigated the interrelationship between LST, NDVI, NDBI, and land cover changes in Amuwo-Odofin, Lagos, Nigeria, using Landsat imagery from 2002 to 2019. The study showed a negative correlation between LST and NDVI and between NDVI and NDBI. The analysis reviled that the NDVI and LST changes are driven by the built-up area expansion. (Ferreira and Duarte, 2019) studied the correlation of urban morphology (Local Climate Zones (LCZ)) and LST in Sao Paulo. The study revealed an inverse relationship between day and night LST with vegetation. It also emphasised that building area and impervious surface have a positive relationship with LST at night, but pervious surface is negatively related. This study has effectively operationalized LCZ in a subtropical context and provides key lessons for the climate-sensitive urban design. Yet the accuracy of the LCZ map was 68% but several LCZ classes were estimated with much error which could lead to biased correlation findings. Zhibin et al. (2015) demonstrate the effect of spatial arrangement of urban greenery on LST. The study suggests that even the green patches are not increased in number but greater aggregation and cohesion of vegetation patches reduce the LST. Anbazhagan and Paramasivam (2016) explored the statistical relationship between LST and NDVI in India's Salem magnesite mining zone, using Landsat TM data from 1992, 2001, and 2010. Their key contribution revealing an inverse correlation where increased emissivity coincided with negative NDVI anomalies. B values for NDVI and LST were consistently negative across the all the years studied (-0.209 in 1992, -0.143 in 2001, and -0.190 in 2010), confirming high LSTs in mining areas due to sparse vegetation and high soil emissivity. Anbazhagan and Paramasivam (2016) validated the satellite-derived LST results against India Meteorological Department (IMD) ground observations. This study does not address the effects of variables such as rain, urbanization on NDVI. The paper by Zhan et al. (2013) critically reviews disaggregation of LST, identifying Thermal Sharpening (TSP) and Temperature Unmixing (TUM) as primary subtopics. A key contribution is its comprehensive taxonomic classification of existing research and insights into future research directions. However, limitations include the field's disorderly development, a lack of citation for foundational works, and challenges arising from unrealistic assumptions regarding surface properties and aggregation patterns, which collectively hinder algorithm improvement and the accuracy of disaggregated LST products.

While numerous studies assess the association between vegetation indices (VI) and land surface

temperature (LST), most work is constrained by fine-resolution data, limited temporal coverage or a single season analysis especially in monsoon-dominated regions. Further, long-term and seasonally-specific investigation on the mining and urbanization affected landscapes of eastern Maharashtra is still limited. This study fills this gap by applying a multi-temporal (2014-2022) vegetation dynamics and LST analysis over part of eastern Maharashtra which is not yet considered for study, with an explicit separation of the pre- and post-monsoon stages.

The eastern part of Maharashtra, particularly around Chandrapur, comprises a diverse and resource-rich landscape, including a wildlife sanctuary, extensive forest cover, mining zones, urban and rural settlements, etc. This area has undergone extensive ecological transformations over the past few decades, largely due to mining, industrialization, urbanization, etc. Therefore, a thorough investigation is required to analyze the correlation between the vegetation cover changes and the LST dynamics. These statistical insights will be advantageous for formulating effective strategies for future vegetation ecosystem restoration and management planning. This study aims to assess the trend of vegetation change and its temperature implication in the Eastern Maharashtra region (2014-2022). The novelty of the study is to apply LULC transition analysis combined with adaptive NDVI-based vegetation classification for studying vegetation-temperature dynamics. Based on combination of seasonal NDVI, LST and land-use classes, the vegetation cooling effect is characterized specifically for the region and urban heat dynamics. The study advances the knowledge of surface temperature and vegetation interaction within the research area. The primary objectives are to

1. Evaluate the seasonal variation in vegetation dynamics using NDVI
2. Compute the change in LST between 2014-2022
3. Estimate the correlation between vegetation and LST fluctuation for the study area over the period, considering seasonal variation

These objectives lay the foundation for the following hypothesis:

H_0: There is a negative relationship between vegetation changes and LST variations during the study period.

H_1: There is a no/positive correlation between vegetation dynamics and LST over the study period.

The major contribution of this study is to analyze temporal variation in vegetation and assess their potential correlation with fluctuations in LST for the study area during pre- and post-monsoon seasons.

2. METHODOLOGY

Figure 1 shows the high-level implementation overview of the proposed workflow. For the time series analysis of the vegetation and LST change detection, Landsat 8 OLI satellite images are retrieved from the Google Earth Engine (Kumar and Mutanga, 2018). The initial phase of the study involves defining the spatial and temporal parameters. The spatial parameters include selection of the study area, and the temporal parameter includes selection of study duration.

The study area shown in Figure 2, includes the eastern part of the Maharashtra state bounded by 19°40’48″ N to 20°18’1″ N latitude and longitude from 78° 52′ 12″ E to 79° 37′ 48″ E, which is imported by considering a geospatial boundary from Google Earth Engine. Concurrently, the temporal window is established between 2014-2022 with an interval of 4 years.

Vegetation and surface temperature behaviour differ for post- and pre-monsoon seasons (Sinha et al., 2019). Hence, to capture medium-term changes, GEE’s Landsat 8 Surface Reflectance Tier 1 Image Collection images for the month of May are considered for pre-monsoon analysis, while November images are considered for post-monsoon analysis. Table 1 gives the detailed information about the collected Landsat 8 images. The area of interest is delimited by the study area boundary polygon. Theses satellite images undergo various pre-processing techniques like Filtering, Radiometric Correction, Spectral Band selection, NDVI calculation, Mosaicking.

Landsat-8 Collection-2 Tier-1 Surface Reflectance imagery, used for this study incorporates Land Surface Reflectance Code based atmospheric correction scheme. This corrects the effects of atmospheric gases, aerosols, and water vapor using auxiliary atmospheric data. This preprocessing step ensures radiometric consistency across multi-temporal observations and is particularly suitable for long-term vegetation and surface temperature analysis. Radiometric calibration is applied to convert the raw digital numbers (DN) into top-of-atmosphere (TOA) reflectance. Pixel-level quality control was performed using the QA_PIXEL band. QA_PIXEL band is a bit-encoded quality assurance layer that flags cloud, cloud

shadow, and cirrus contamination. Cloud-affected pixels were identified through bitwise evaluation of cirrus (bit 2), cloud shadow (bit 3), and high-confidence cloud flags (bit 5) and were excluded from further analysis. Based on these criteria, a binary cloud mask M(x) indicated by Equation 1 was generated for each pixel x, retaining only clear-sky observations and thereby minimizing atmospheric artefacts. This mask minimizes cloud-induced radiometric distortion. This conservative masking strategy is particularly important for monsoon-affected regions such as eastern Maharashtra, where residual cloud contamination can significantly bias surface reflectance and land surface temperature estimates.

$$M(x) = \begin{cases} 1 \text{ if bits cirrus (bit 2), shadow (bit 3), and cloud (bit 5) all are 0} \\ 0 \text{ Othereise} \end{cases} \quad (1)$$

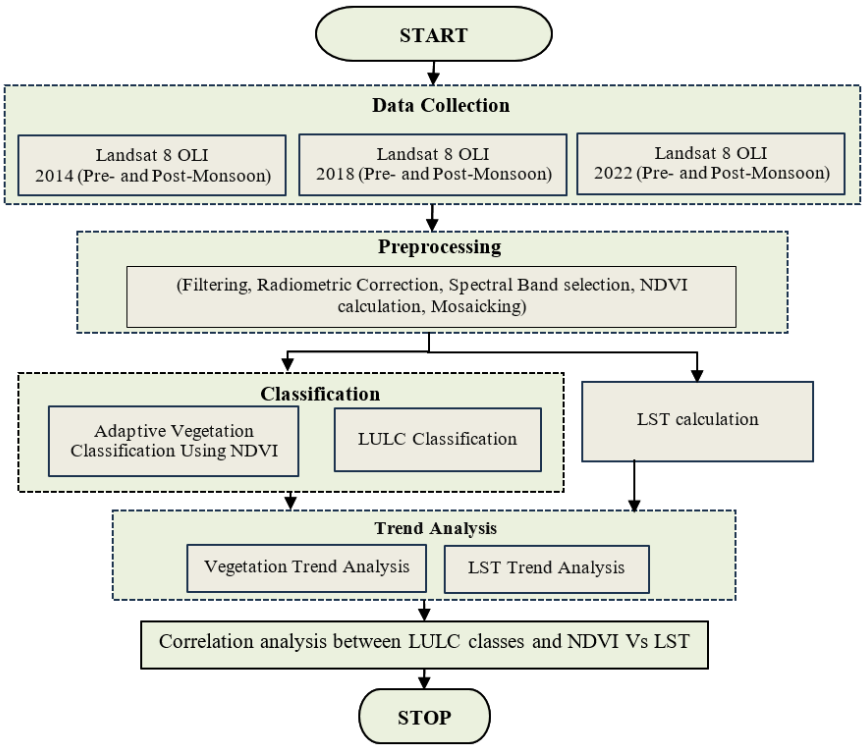

Figure 1. Overview of implementation

Figure 2. Study area covering eastern part of the Maharashtra state

Table 1. Data description of Landsat 8 remote sensing data acquired for study area

Season	Year	Date of acquisition	Path-row	Resolution of visible and near infrared band (m)	Resolution of TIR (m)
Pre-Monsoon	2014	2014-05-11	143-045	30	100
Post-Monsoon	2014	2014-11-19	143-045	30	100
Pre-Monsoon	2018	2018-05-13	143-045	30	100
Post-Monsoon	2018	2018-11-14	143-045	30	100
Pre-Monsoon	2022	2022-05-17	143-045	30	100
Post-Monsoon	2022	2022-11-16	143-045	30	100

This excludes pixels of the mask and improves data quality for further analysis. To cover the large study area, through mosaicking images are stitched together to provide complete study area. Landsat 8 imagery has total 11 bands and each band contain the specific information. For the study, careful band selection is carried out and specific spectral bands like band 4 (red), band 5 (near-infrared (NIR)), and band 10 (the thermal infrared (TIR)) are extracted. The TIR band is used for estimating Land Surface Temperature (LST), while the reflectance of red and NIR bands are used to calculate Normalized Difference Vegetation Index (NDVI), which is utilized to estimate the vegetation cover. Equation 2 is used to calculate the NDVI index (Hutayanon and Somprasong, 2023). Later, NDVI is stacked as a new band in the image.

$$\mathrm{NDVI} = \frac{\mathrm{NIR}-\mathrm{RED}}{\mathrm{NIR}+\mathrm{RED}} \quad (2)$$

Where; NIR: Reflectance of the NIR band; RED: Reflectance of the Red Band.

The value of NDVI ranges between -1 and +1. The non-positive NDVI value is indicative of a non-vegetated surface, while a positive value corresponds to the vegetated area (Garai et al., 2022). The increasing value of NDVI reflects greater vegetation density (Gandhi et al., 2015).

Equation 3 specifies the criteria to perform adaptive classification using NDVI values. Adaptive classification applies percentile-based thresholds to classify vegetation into categories such as no vegetation, sparse, moderate, and dense cover. The method allows context-sensitive interpretation that adjusts to each image's NDVI distribution.

$$C(x,y) = \begin{cases} C1 & \text{if } \mathrm{NDVI}(x,y) \le P_{10} \\ C2 & \text{if } P_{10} < \mathrm{NDVI}(x,y) \le P_{50} \\ C3 & \text{if } P_{50} < \mathrm{NDVI}(x,y) \le P_{85} \\ C4 & \text{if } \mathrm{NDVI}(x,y) > P_{85} \end{cases} \quad (3)$$

Where; C(x,y): Classified output at pixel (x,y); NDVI(x,y): NDVI value at Pixel (x,y); P_{10} , $P_{50,}$ P_{85}: 10^{th}, 50^{th}, 85^{th} percentiles of the NDVI array; C1: No vegetation class, C2: Sparse vegetation Class, C3: Moderate vegetation Class, and C4: Dense vegetation class.

This NDVI value is further used for land use classification and classified the region in three classes namely Water, Vegetation and Built-up land. Equation 4 represents the classification function L(x,y).

$$L(x,y) = \begin{cases} 1 & \text{if } \mathrm{NDVI}(x,y) < 0 \quad (\mathrm{Water}) \\ 2 & \text{if } \mathrm{NDVI}(x,y) > 0.2 \quad (\mathrm{Built-up}) \\ 3 & \text{if } 0 \le \mathrm{NDVI}(x,y) \le 0.2 \ (\mathrm{Vegetation}) \\ \mathrm{NaN} & \text{if } \mathrm{NDVI}(x,y) = \text{Undefined or masked value} \end{cases} \quad (4)$$

Where; NDVI(x, y) ∈ R denotes the NDVI at the spatial location (x, y). R is a set of real number. L(x, y) ∈ {1, 2, 3} ∪ {NaN}, denotes land use function where 1 represents water, 2 represents vegetation, 3 represents built-up / bare Land, NaN indicates undefined or masked values.

Further, the land surface temperature is calculated using the TIR band (García-Santos et al., 2018). The emitted thermal radiations are represented by the pixel-level digital numbers (DN) of this band. After calibration, these DNs are converted into the surface temperature values using a scale factor and additive offset. This transformation is applied using Equation 5.

$$\mathrm{LST}_{\mathrm{KELVIN}} = (\mathrm{T\_B10} \times \mathrm{Scale\_Factor}) + \mathrm{Offset} \quad (5)$$

Where; ST_B10: Landsat 8 satellite images's Band 10 pixel value represented as digital number. Scale_Factor=0.00341802; Offset =149.0.

The scale factor adjusts the magnitude of DN to align with radiometric calibration, while the offset corrects the baseline to reflect absolute temperature values. Once the temperature values in Kelvin are obtained, they are converted to degrees Celsius using Equation 6.

$$LST_{Celsius} = LST_{KELVIN} - 273{,}15 \quad (6)$$

To understand the correlation between various land covers and LST, correlation is calculated using Equation 7.

$$C_r = \frac{Cov(a,b)}{\sigma_a \sigma_b} \quad (7)$$

Where; a: the land class value array; b: LST value arrays; Cov(X,Y): the covariance between land cover class and LST; σ_a, σ_b: the standard deviations of land cover class and LST respectively.

The present study relies exclusively on data derived from the Landsat 8 satellite imagery. No in-situ temperature measurements, field-based vegetation assessments, or meteorological station records were available for direct validation of the NDVI and LST products used in this analysis. Hence to explore sensor or algorithm-dependent bias, a cross-sensor evaluation is caried out with MODIS land surface temperature products (Meshesha et al., 2024). The MODIS MOD11A2 data set provides 8 days composite daytime LST at 1 km spatial resolution, retrieved using a split-window algorithm, and was used as an independent reference to assess the robustness of the Landsat-derived LST estimates. LST of Landsat 8 was acquired from its thermal infrared band using a single-channel method, then resampled and aggregated spatially to the MODIS scale (1 km) in order to minimize the differences caused by scales. A pixel-wise statistical comparison was carried out over the entire study area for a pre-monsoon period (May 2022). The corresponding Pearson correlation coefficient was 0.72, representing a strong positive linear relationship and the presence of high-level consistency in spatial temperature patterns among sensors. The average bias was 1.6°C point out a small systematic shift and Landsat-derived LST values are slightly higher on average. The RMSE of 2.4°C belongs to the uncertainties that are frequently reported for cross-sensor LST comparisons. Taken together, these statistics enforce that the LST estimates derived from Landsat data are not dominated by sensor or algorithm specific artifacts and provide confidence in their use for subsequent NDVI-LST relationship analysis.

3. RESULTS AND DISCUSSION

The first objective of this study is to analyse the vegetation dynamics from 2014 to 2022 using the vegetation index. Figure 3 represents the NDVI analysis for the study area for pre- and post-monsoon seasons.

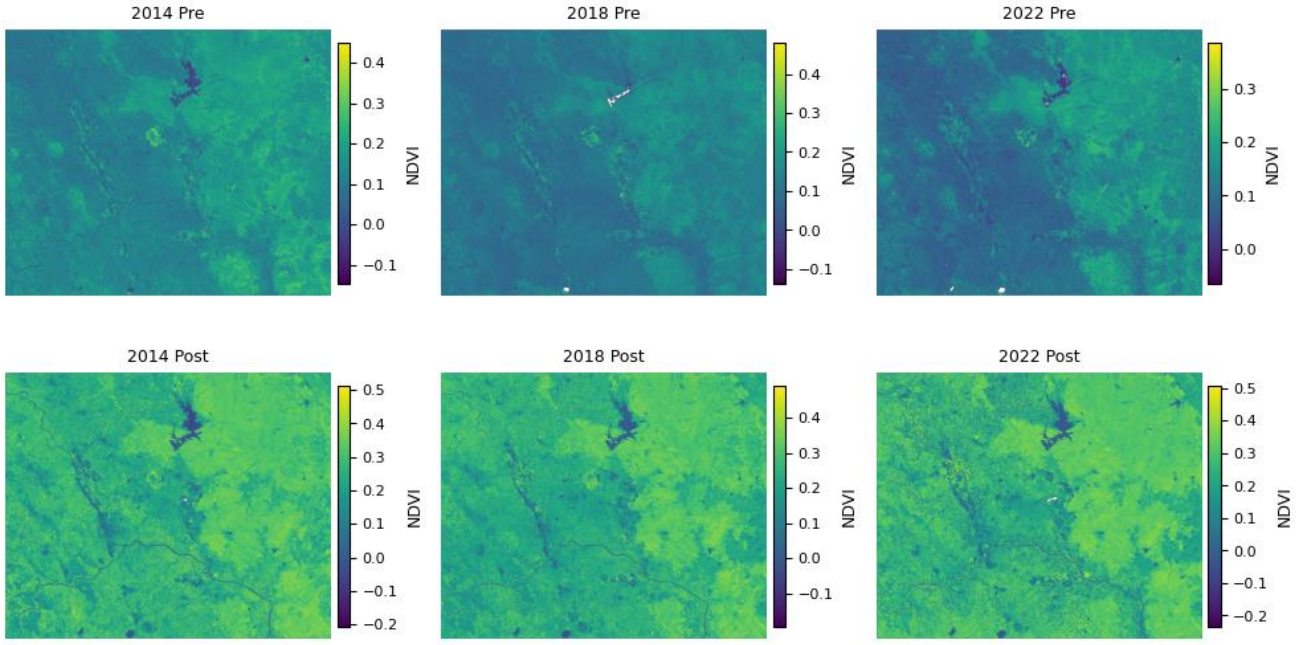

Figure 3. NDVI map for the study area for the year 2014, 2018, and 2022

The statistical NDVI information derived from remote sensing data for the post-monsoon and pre-monsoon periods for the years 2014, 2018, and 2022 is included in Table 2. For each year, the average, minimum, and maximum values for the pre- and post-monsoon periods are considered for further analysis.

The average NDVI value for the pre-monsoon was 0.145810 (range: -0.146479 to 0.450364) in 2014, and the average NDVI value for the post-monsoon was 0.264453 (range: -0.205797 to 0.5131). In 2018, the pre-monsoon NDVI mean was 0.121021 (range: -0.136576 to 0.480856), and the post-monsoon NDVI mean increased to 0.246208 (range: -0.194962 to 0.491923) similarly. In 2022, the NDVI value was averaged to 0.127531 (range: -0.064556 to 0.386672) during the pre-monsoon period and 0.255649 (range: -0.233793 to 0.508318) during the post-monsoon period. Across all three years, average NDVI values during post-monsoon are consistently higher than their pre-monsoon counterparts. This observation justifies the natural vegetation trend of a rise in the sprawl following the monsoon season.

Figure 4 give details about the temporal analysis of vegetation change dynamics based on average NDVI value for years 2014, 2018, and 2022 during pre- and post-monsoon season.

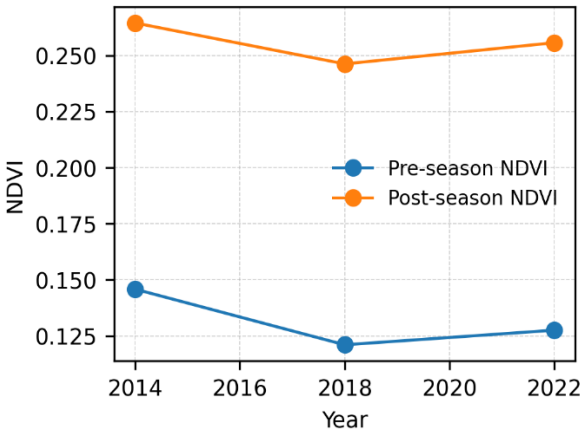

Figure 4. Average NDVI pre Vs post monsoon season analysis from 2014 to 2022

Table 2. Statistical comparison of pre- and post-monsoon NDVI values

Year	Pre-Monsoon				Post-Monsoon			
	Maximum	Minimum	Average	Standard deviation	Maximum	Minimum	Average	Standard deviation
2014	0.450364	-0.146479	0.145810	0.049396	0.513100	-0.205797	0.264453	0.071778
2018	0.480856	-0.136576	0.121021	0.038752	0.491923	-0.194962	0.246208	0.066222
2022	0.386672	-0.064556	0.127531	0.045665	0.508318	-0.233793	0.255649	0.083301

The pre-season NDVI, representing vegetation conditions before the growing season, shows a noticeable decline in 2018, followed by a slight recovery in 2022. This trend suggests increasing environmental stress during this period. The post-season NDVI, indicating the status of vegetation after the monsoon season, exhibits a constant decline. Though post-season NDVI values are higher than pre-season values (in accordance with seasonal growth), the overall decrease in both indicates a decrease of vegetation productivity and health over time. Such a decline could be related to reasons like land degradation, climatic stress, and agricultural intensification. A decreasing trend in the difference between pre- and post-season NDVI implies decreasing seasonal vegetative cover recovery, which may affect ecosystem functions like soil retention, evapotranspiration, and carbon storage.

The adaptive NDVI percentile value-based classification maps for the years 2014, 2018, and 2022, shown in Figure 5, use a consistent colour scheme to highlight spatial and temporal patterns of vegetation cover. Context-sensitive assessments of vegetation cover are possible using dynamic percentile thresholds (P10, P50, and P85) based on vegetation classification. Seasonal transitions are distinctly highlighted in all three years, where sparse to moderate vegetation dominates during pre-monsoon periods with considerable areas devoid of vegetation cover, which was predominant in 2014 and 2022. Post-monsoon maps show substantial increases in moderate and dense vegetation classes compared to pre-monsoon sparse vegetation dominance. Also, the landscape greening observed from pre- to post-monsoon periods is supported by significant rises in percentile value such as P50 and P85. As depicted in Figure 5, the extended range of dense vegetation compared to moderate vegetation observed in the 2022 map indicates improved vegetative health for that year, likely due to better land management. These maps emphasize interannual variability with intraseasonal change while demonstrating adaptive classification's advantages for monitoring dynamics of vegetation cover over time.

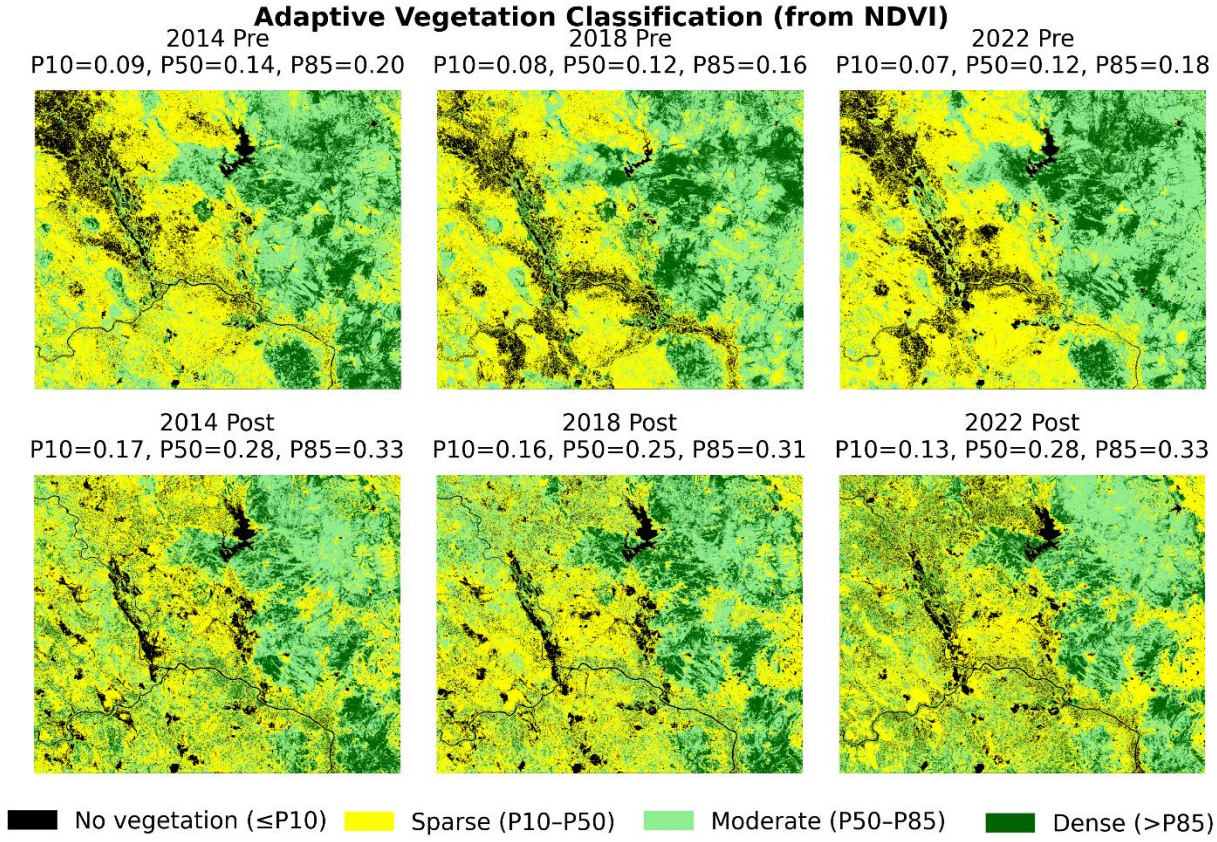

Figure 5. Vegetation distribution analysis using NDVI based adaptive classification for the years 2014, 2018, and 2022

This spatial interpretation of vegetation dynamics is further supported by the transition matrices shown in Figure 6. It quantifies changes in different vegetation classes from pre- to post-monsoon seasons. This helps in understanding the extent of vegetation cover change across years. For all three years, the common pattern is followed where a large part of the low vegetation area during the pre-monsoon turns into a moderate vegetation area post-monsoon. In 2014, 47.0% of the region was converted from low to moderate vegetation.

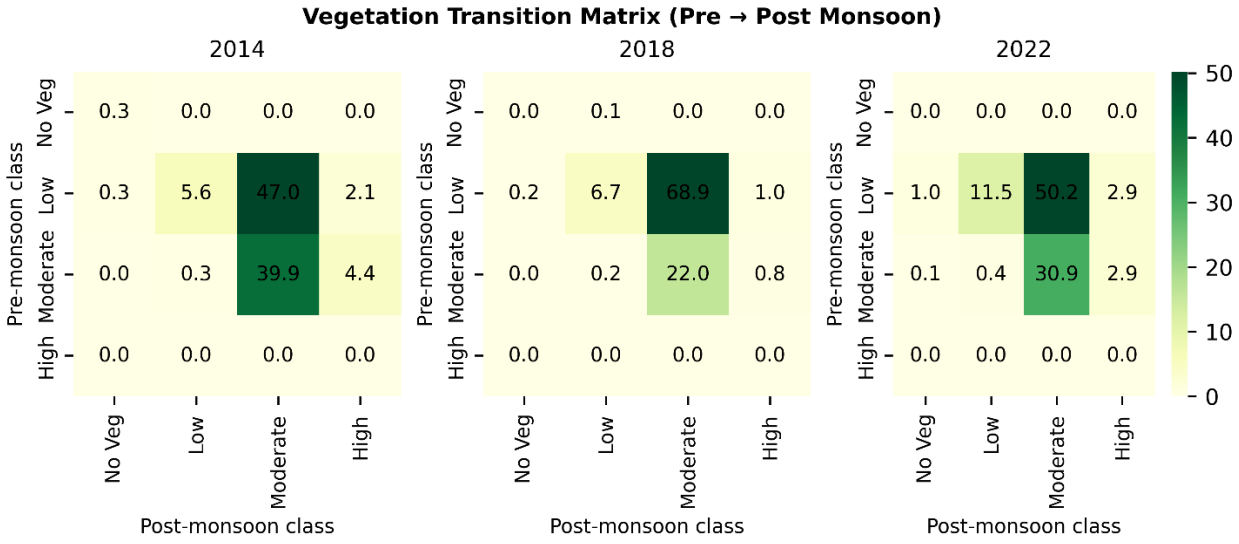

Figure 6. Year wise pre vs post monsoon transition matrix for different vegetation classes

The conversion level improved in 2018 and showed a 68.9% transition from low to moderate vegetation, representing a more intense greening effect. The year 2022 has also shown a strong low-to-moderate transition (50.2%) and an interesting appearance of 2.9% transitioning from moderate to high vegetation, which was very low in 2018. Overall, these matrices confirm the expected seasonal vegetation dynamics, where NDVI values increase after the monsoon, and also highlight an encouraging shift in 2022 toward higher vegetation classes.

To understand transition of vegetation class with other LULC classes, LULC classification is carried out. As mention in the Table 3, overall accuracy of the LULC classification was 89.04% and Kappa coefficient was 0.86, indicating strong agreement. Vegetation and water classes are highly reliable, whereas the user's accuracy for the built-up class is lower indicating it's confusion with bare land and sparsely vegetated areas. This may add some noise to NDVI based classification but does not affect the general seasonal trend.

Table 3. Accuracy assessment for LULC classification

Class	User's accuracy (%)	Producer's accuracy (%)
Vegetation	88.70	90.21
Built up	84.64	87.01
Water	90.42	92.36
Overall accuracy (%)	89.04	
Kppa coefficient	0.86	

Figure 7 presents pre- and post-monsoon LULC transitions for the years 2014, 2018, and 2022, expressed as a percentage change. A substantial proportion of built-up land areas identified during the pre-monsoon season transition to the vegetation class in the post-monsoon period across all three years (68.95% in 2014, 75.27% in 2018, and 71.18% in 2022). This shift reflects a pronounced post-monsoon greening effect rather than actual anthropogenic land-cover change.

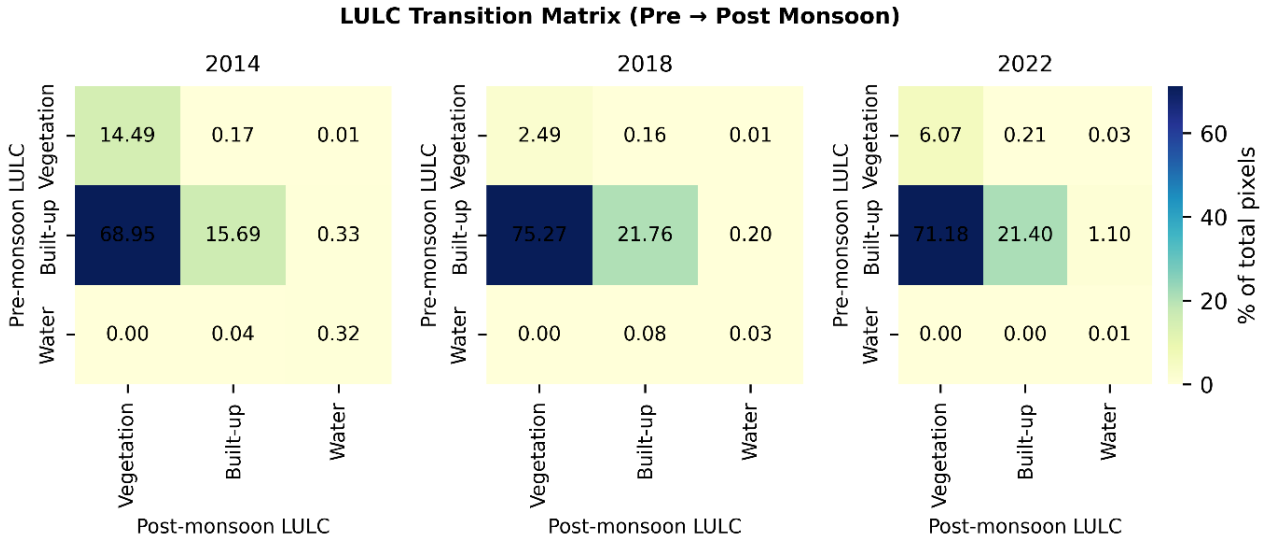

Figure 7. Year wise pre vs post monsoon transition matrix for different LULC classes

The overall vegetation analysis ascertains that in monsoon-influenced environments, seasonal vegetation growth over bare soils, mining spoils, road margins, and peri-urban vacant land increases surface greenness and leads to spectral mixing at the 30 m spatial resolution of Landsat. Consequently, mixed pixels containing impervious surfaces partially obscured by seasonal vegetation are frequently misclassified as vegetation during the post-monsoon season. This phenomenon represents seasonality-driven vegetation obscuration of built-up surfaces and is a well-documented limitation in medium-resolution

optical remote sensing analyses (Arij et al., 2025). The low values for the Water class to/from status in all years indicate stable water bodies. The vegetation-to-vegetation class change is especially important, moving from 14.49% in 2014 to 2.49% in 2018, to then increase back to 6.07% in 2022, which suggests the temporal variability of the persistence of vegetal cover, probably. Investigations into the underlying climatic or anthropogenic factors responsible for the temporal pattern are therefore necessary.

The identified interannual trend in NDVI, for the period 2014-2018, is indicative of anthropogenic activity and other climatic drivers (Rahimi et al., 2025; Zhang et al., 2022). The increasing mining activities, industrial infrastructure and expanded urbanization have transformed the vegetated area into built-up and bare land. This observed a trend in study area has been regularly recorded in minerally-dominated and rapidly developing landscapes (Anbazhagan and Paramasivam, 2016). These changes of land cover decrease the grass cover, exposing the surface for evapotranspiration and promote the rise in LST (Zhibin et al., 2015; Ferreira and Duarte, 2019). Moreover, frequent pre-monsoon heat stress limits the vegetation growth (Nassif et al., 2023; Sinha et al., 2019). This act as strong evidence for the finding for this study stating vegetation declination and LST rise in pre-monsoon season. Despite the fact that post-monsoon NDVI values are higher than pre-monsoon ones because of season-based greening, such a steady long-term decrease suggests a slow deterioration in vegetation productivity and ecosystem resilience (Psistaki et al., 2024). The partial recovery in 2022, especially in dense vegetation classes, might be owing to favourable monsoon conditions and local land administration practices but even such short-term improvements are not enough to counteract the long-term degradation (Gandhi et al., 2015; Ullah et al., 2023). Moreover, frequent pre-monsoon heat stress and enhanced variability in rainfall restrict growth of vegetation while keeping a check on the seasonal recovery as well (Nassif et al., 2023; Sinha et al., 2019).

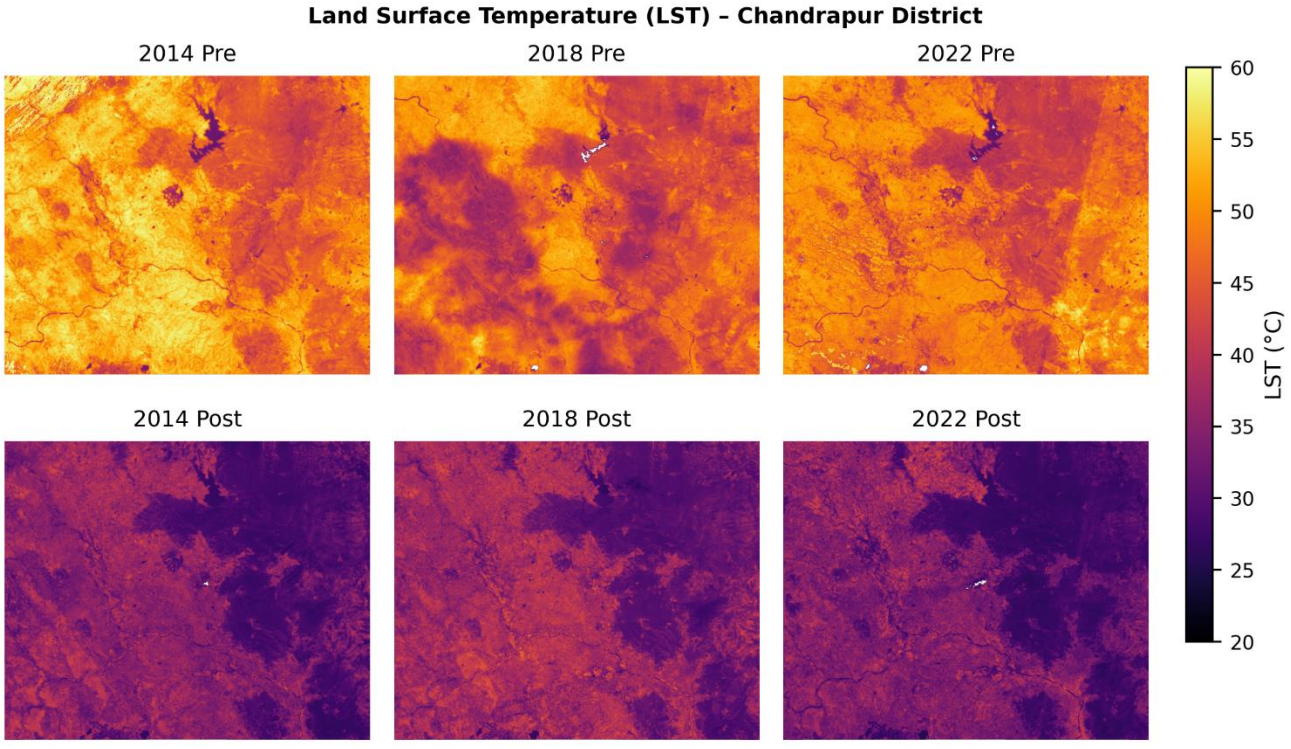

Figure 8. LST map for the study area for the years 2014, 2018, and 2022

The objective 2 focuses on computing LST. Figure 8 represents the LST map for the study area, while Table 4 presents statistics for the average, the minimum, and the maximum pre-monsoon-post-monsoon LST for 2014, 2018, and 2022. The average LST for the pre-monsoon in 2014 was 49.73 (range: 26.09-63.84) and for the post-monsoon average was lower than that, at 33.24°C (range: 23.91°C-48.42°C). In 2018 the same trend was followed: pre-monsoon mean LST was 44.70°C (range: 28.82°C-59.87°C), which reduced in post-monsoon to 35.20°C (range: 3.98°C-50.30°C). In 2022, the pre-monsoon mean was

46.91°C (range: 22.78°C-60.22°C), and post-monsoon decreased to 32.21 (range: 25.02°C-47.47°C). Between the three years, post-monsoon mean LST is always less than pre-monsoon mean LST. This means there has been a significant decrease in LST following the monsoon season.

Table 4. Statistical comparison of pre- and post-monsoon LST values

Year	Pre-monsoon LST (°C)				Post-monsoon LST (°C)			
	Maximum	Minimum	Average	Standard deviation	Maximum	Minimum	Average	Standard deviation
2014	63.84	26.09	49.73	4.86	48.41	23.91	33.24	3.66
2018	59.87	28.82	44.70	4.49	50.30	3.98	35.20	3.81
2022	60.22	22.78	46.91	3.93	47.47	25.02	32.21	3.68

Figure 9 shows a time series analysis of LST for 2014, 2018, and 2022 and depicts the comparison of the LST just before and just after monsoon. The pre-season LST in 2014 was high, hinting that the ground was much hotter than usual for that stage of the year. By 2018 that same early figure dropped, pointing to a brief cooling spell probably linked to kinder weather. Yet 2022 brought the pre-season LST back up, suggesting renewed heating likely caused by tree loss, spread of pavement, and other signs of growing development. The post-monsoon LST creeps up in both 2014 and 2018 before sliding down in 2022.

Even so, every year, the early-season temperature is still above the late-season figures by a healthy margin. That pattern fits what we expect—gaps in vegetation at the start of the season let sunlight warm the ground more, while denser post-season plants cool things down through evaporation. Oddly though, those post-season readings in 2014 and 2018 lingered a bit above the long-term average before the slight drop seen in 2022.

The third study objective is inclined toward investigating the potential relationship between vegetation change and land surface temperature fluctuation over the study period. Table 5 presents the relation between land cover classes and LST by considering the correlation of LST with land cover classes (water, vegetation, and built-up) and the overall correlation of NDVI-LST for the pre-monsoon and post-monsoon seasons for 2014, 2018, and 2022. Vegetation cover has a consistently moderate to strong negative relationship with LST, indicating the cooling effects due to evapotranspiration. The urban buildup and LST showed a positive correlation with higher surface temperatures in built-up areas, indicating the urban heat island effect. Water does exhibit weak negative correlations, which may result from localized extents or mixed pixels. The overall correlation of NDVI-LST is still strongly negative, indicating that increased vegetation density is correlated with reduced surface temperature.

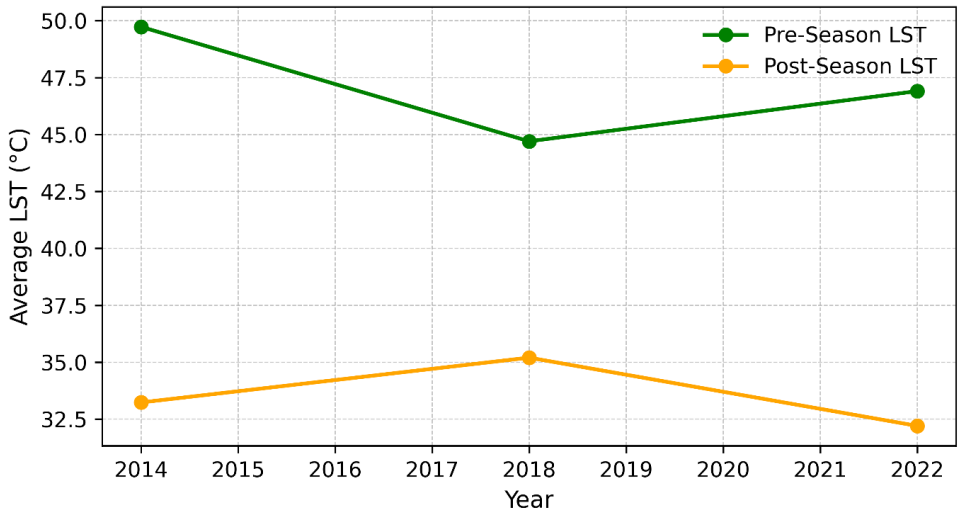

Figure 9. Average LST pre- Vs post-monsoon season analysis from 2014 to 2022

Table 5. LST Correlation between LULC classes and overall NDVI values for pre and post monsoon season

Season-year	Water vs. LST correlation	Vegetation vs. LST correlation	Built-up vs. LST correlation	Overall NDVI vs. LST correlation
Pre-monsoon 2014	-0.170594	-0.446206	0.470401	-0.603048
Post-monsoon 2014	-0.113006	-0.382907	0.414315	-0.557735
Pre-monsoon 2018	-0.060394	-0.143083	0.152460	-0.253942
Post-monsoon 2018	-0.058556	-0.411356	0.420279	-0.569535
Pre-monsoon 2022	-0.019580	-0.313470	0.314058	-0.513839
Post-monsoon 2022	-0.127817	-0.457682	0.500331	-0.530829

This observed inverse pattern does support the null hypothesis (H_0), which states that higher levels of vegetation lead to decreasing LST and vice versa. The results shows empirical evidence that the change in vegetation causes cooling of the surface temperature in the study area. We reject the alternative hypothesis (H_1), which says there is a positive relationship.

These findings have direct policy relevance, underscoring the need for vegetation-centered land-use planning, afforestation initiatives, mine reclamation strategies, and the integration of green infrastructure into regional development frameworks. The results provide a quantitative basis for promoting nature-based solutions aimed at mitigating heat stress and enhancing climate resilience in rapidly transforming landscapes.

4. LIMITATIONS AND FUTURE DISCUSSION

A key limitation of this study is the absence of ground-based or station-based validation data. NDVI and LST estimates were derived solely from Landsat 8 satellite imagery, and no site-specific land temperature observations, field-based vegetation measurements, or meteorological station records were available for direct verification. This limitation may introduce uncertainty in the absolute accuracy of the NDVI values. Despite this limitation, satellite-derived NDVI and LST products have been extensively validated in previous studies and are widely accepted for regional-scale environmental monitoring and trend analysis.

Future extensions of this work will aim to integrate meteorological station air temperature data, field-based vegetation indicators to further strengthen confidence in absolute estimates. The current study is based on the 30m spatial resolution imagery which may contribute to mixed pixels, and classification errors. In future finer spatial resolution can be used for better results.

5. CONCLUSION

The present study analysed vegetation dynamics and land surface temperature change taking place in Eastern Maharashtra during the period of 2014-2022 with the help of Landsat 8 imagery queried from Google Earth Engine. Inline to the first study objective, the results consistently reveal the higher average NDVI values of post-monsoon periods that yield lower LSTs than pre-monsoon periods, reconfirming the seasonally predictable growth patterns and the cooling nature of vegetation. Although a general pattern of negative vegetation productivity and health over the study period was observed, but as per the Figure 5 a remarkable improvement of dense vegetation classes was observed in 2022, possibly a positive influence resulting from improved land management or favourable climatic conditions. Addressing Objective 2, the temporal assessment of LST revealed a clear seasonal and interannual variability over the study period. Consistent with objective 3, the correlation test supported the null hypothesis (H_0) and showed a negative moderate to strong relationship between NDVI and LST, thus emphasizing the important role of transpiration in mitigating surface temperatures. In contrast, the built-up land areas were positively correlated with LST, reflecting the urban heat island effects. The transition matrices were informative as to discovering land cover changes, although this did pose questions about possible spectral confusion. This study provides insight into the vegetation-thermal environment relationship at a regional scale in a tropical area, which gives important insights for environmental monitoring and management strategy in such regions. Future investigations could entail integrating more climatic variables, seeking out finer spatial-temporal scales, and conducting more localized studies to identify specific anthropogenic and natural drivers of observed changes.

ACKNOWLEDGEMENTS

The authors would like to acknowledge the KJ Somaiya School of Engineering for providing the computing facilities.

AUTHOR CONTRIBUTIONS

All authors agreed on the content of the study. Dipti Pawade (DP) and Sonali Patil (SP) conceptualized the initial research concept and plan of intervention. DP and SP cooperatively did the literature search and conceived the design and methodology of the study. DP carried out the data collection and did the analysis. DP and SP collectively interpreted the results as well as prepared, edited, reviewed, and approved the manuscript.

DECLARATION OF CONFLICT OF INTEREST

The authors declare no competing interests.

REFERENCES

Alademomi AS, Odumosu J, Okolie CJ, Daramola OE, Akinnusi SA, Adediran E, et al. The interrelationship between LST, NDVI, NDBI, and land cover change in a section of Lagos metropolis, Nigeria. Applied Geomatics 2022;14:299-314.

Anbazhagan S. Paramasivam CR. Statistical correlation between land surface temperature (LST) and vegetation index (NDVI) using multi-temporal Landsat TM Data. International Journal of Advanced Earth Science and Engineering 2016;5:333-46.

Arij N, Latifi H, Fakhri A, Esmaili R. Four decades of spatio-temporal trends in Miankaleh Wetland's water body and vegetation as revealed by remote sensing time series. Ecological Informatics 2025;91:Article No. 103374.

Bandh SA, Shafi S, Peerzada M, Rehman T, Bashir S, Wani SA, et al. Multidimensional analysis of global climate change: A review. Environmental Science and Pollution Research 2021;28:24872-88.

Ferreira LS, Duarte DHS. Exploring the relationship between urban form, land surface temperature and vegetation indices in a subtropical megacity. Urban Climate 2019;27:105-23.

De Frenne P, Lenoir J, Luoto M, Scheffers BR, Zellweger F, Aalto J, et al. Forest microclimates and climate change: Importance, drivers and future research agenda. Global Change Biology 2021;27:2279-97.

Gandhi GM, Parthiban S, Thummalu N, Christy A. Ndvi: Vegetation change detection using remote sensing and Gis - A case study of Vellore District. In: Procedia Computer Science, Vol. 57. Elsevier; 2015. p. 1199-210.

Garai S, Khatun M, Singh R, Sharma J, Pradhan M, Ranjan A, et al. Assessing correlation between Rainfall, normalized difference Vegetation Index (NDVI) and land surface temperature (LST) in Eastern India. Safety in Extreme Environments 2022;4:119-27.

García-Santos V, Cuxart J, Martínez-Villagrasa D, Jiménez MA, Simó G. Comparison of three methods for estimating land surface temperature from Landsat 8-TIRS Sensor data. Remote Sensing (Basel) 2018;10(9):Article No. 1450.

Hutayanon T, Somprasong K. Application of integrated spatial analysis and NDVI for tree monitoring in reclamation area of coal mine. Environmental Science and Pollution Research 2023;32:13053-63.

Islam S, Karipot A, Bhawar R, Sinha P, Kedia S, Khare M. Urban heat island effect in India: A review of current status, impact and mitigation strategies. Discover Cities 2024;1:Article No. 34.

Kumar D, Shekhar S. Statistical analysis of land surface temperature-vegetation indexes relationship through thermal remote sensing. Ecotoxicology and Environmental Safety 2015;121:39-44.

Kumar L, Mutanga O. Google Earth Engine applications since inception: Usage, trends, and potential. Remote Sensing (Basel) 2018;10:Article No. 1509.

Li M, Bai Q, Du W. The world is different because of you: Global warming, technological progress and economic development. Structural Change and Economic Dynamics 2025;74:202-11.

Li ZL, Wu H, Duan SB, Zhao W, Ren H, Liu X, et al. Satellite remote sensing of global land surface temperature: Definition, methods, products, and applications. Reviews of Geophysics 2023;61:e2022RG000777.

Longobardi P, Montenegro A, Beltrami H, Eby M. Deforestation induced climate change: Effects of spatial scale. PLoS One 2016;11(4):e0153357.

Meshesha KS, Shifaw E, Kassaye AY, Tsehayu MA, Eshetu AA, Agegnehu HW. Evaluating the relationship of vegetation dynamics with rainfall and land surface temperature using geospatial techniques in South Wollo Zone, Ethiopia. Environmental Challenges 2024;15:Article No. 100895.

Nassif WG, Lagenean FHS, Al-Taai OT. Impact of vegetation cover on climate change in different regions of Iraq. Caspian Journal of Environmental Sciences 2023;21:333-42.

Pawade D, Patil S. Environmental and socio-economic impacts of coal mining in India: A comprehensive analysis. In: Advances in Emerging Technologies and Computing Innovations. Cham: Springer Nature Switzerland; 2025. p. 371-9.

Psistaki K, Tsantopoulos G, Paschalidou AK. An overview of the role of forests in climate change mitigation. Sustainability (Switzerland) 2024;16(14):Article No. 6089.

Rahimi E, Dong P, Jung C. Global NDVI-LST correlation: Temporal and spatial patterns from 2000 to 2024. Environments 2025;12(2):Article No. 67.

Sinha P, Nageswararao MM, Dash GP, Nair A, Mohanty UC. Pre-monsoon rainfall and surface air temperature trends over India and its global linkages. Meteorology and Atmospheric Physics 2019;131:1005-18.

Ullah W, Ahmad K, Ullah S, Tahir AA, Javed MF, Nazir A, et al. Analysis of the relationship among land surface temperature (LST), land use land cover (LULC), and normalized difference vegetation index (NDVI) with topographic elements in the lower Himalayan Region. Heliyon 2023;9:e13322.

Venkataramanan M, Smitha. Causes and effects of global warming. Indian Journal of Science and Technology 2011;4:226-9.

Wei S, He Z, Zhai W, Zhao C, Li Y. How does vegetation influence surface temperature across various road types and urban morphology types? Building and Environment 2025;270:Article No. 112511.

Yuxi W, Li P, Yuemin Y, Tiantian C. Global vegetation-temperature sensitivity and its driving forces in the 21st century. Earths Future 2024;12(2):e2022EF003395.

Zhan W, Chen Y, Zhou J, Wang J, Liu W, Voogt J, et al. Disaggregation of remotely sensed land surface temperature: Literature survey, taxonomy, issues, and caveats. Remote Sensing of Environment 2013;131:119-39.

Zhang L, Yang L, Zohner CM, Crowther TW, Li M, Shen F, et al. Direct and indirect impacts of urbanization on vegetation growth across the world's cities. Science Advances 2022;8(27):eabo0095.

Zhibin R, Haifeng Z, Xingyuan H, Dan Z, Xingyang Y. Estimation of the relationship between urban vegetation configuration and land surface temperature with remote sensing. Journal of the Indian Society of Remote Sensing 2015;43:89-100.